

# **N,N'-Diphenylperylene Diimide Functioning as a Sensitizing Light Absorber Based on Excitation Transfer for Organic Thin-Film Solar Cells**

Musubu Ichikawa<sup>1,2,\*</sup>, Shinya Deguchi<sup>1</sup>, Takashi Onoguchi<sup>1</sup>, Hyeon-Gu Jeon<sup>1,†</sup>, Gilles D. R. Banoukepa<sup>1,3</sup>

<sup>1</sup>*Interdisciplinary Graduate School of Science and Technology, Shinshu University,  
3-15-1 Tokida, Ueda City, Nagano 386-8567, Japan*

<sup>2</sup>*Presto, Japan Science and Technology Agency (JST), 4-8-1 Honcho, Kawaguchi,  
Saitama 332-0012, Japan*

<sup>3</sup>*Japan Society for the Promotion of Science, 8 ichibancho, Chiyoda, Tokyo 102-8472,  
Japan*

(Received )

**Abstract:** We demonstrated that N,N'-diphenylperylene tetracarbonic diimide (PTCDI-Ph) could work as an n-type sensitizing layer for the C<sub>60</sub> n-type layer owing to interlayer excitation transfer (ET) when the PTCDI-Ph layer was placed between the C<sub>60</sub> layer and the aluminum anode coupled with the bathocuproine layer. Well-aligned lowest unoccupied molecular orbitals between C<sub>60</sub> and PTCDI-Ph ( $-4.55$  eV for

PTCDI-Ph and  $-4.5$  eV for C<sub>60</sub>) and a larger bandgap for PTCDI-Ph than C<sub>60</sub> ( $2.04$  eV for PTCDI-Ph and  $2.0$  eV for C<sub>60</sub>) enabled this interlayer ET-based sensitization. Further, the optical interference effect could be also involved in the sensitization. It was also demonstrated that the combination of both n-type materials C<sub>60</sub> and PTCDI-Ph could successfully reduce the amount of the expensive C<sub>60</sub> used, and a thin C<sub>60</sub> layer was indispensable for efficient charge separation. PTCDI-Ph could work as a light-harvesting n-type material incorporating C<sub>60</sub>-based cells to compensate for C<sub>60</sub>'s weak optical absorption.

Keywords: organic photovoltaics, organic solar cells, perylene diimide, fullerene, excitation transfer, sensitization, optical interference

\*Corresponding author at: *Interdisciplinary Graduate School of Science and Technology, Shinshu University, 3-15-1 Tokida, Ueda City, Nagano 386-8567, Japan*

Tel: +81-268-21-5498; Fax: +81-268-21-5417

Email address: musubu@shinshu-u.ac.jp

<sup>†</sup>Present address: *Department of Materials Science and Biotechnology, Graduate School of Science and Engineering, Ehime University, Matsuyama 790-8577, Japan*

## **1. Introduction**

In recent years, organic photovoltaic (PV) cells have emerged as a promising solar cell technology, and the potential to fabricate flexible, lightweight devices with low material consumption and tunable absorption characteristics opens the way to a cost-efficient electricity supply.[1, 2] Increasing research efforts have steadily improved power conversion efficiencies (PCE) in small-molecule-based organic [3-6] and polymer-based [6-10] PV cells since the first efficient bilayer photovoltaic cell was reported by Tang.[11] Structurally well-defined small molecular materials avoid the inherent batch-to-batch physical property variations in polymers, and therefore, provide better reproducibility. In addition, they can be adapted for vacuum evaporation deposition techniques, which allow well-defined layer-by-layer structures to be built. Thus, vacuum evaporation-deposition fabricated organic small-molecule PV cells provide various potential future improvements to the PCE of organic PV cells—improvements which are still needed to make PV cells truly useful.

To enhance PCE, researchers must first increase the efficiency of light absorption and broaden the usable spectrum, which could be achieved by using more than two materials having complementary optical absorption properties. While organic PV cells fundamentally require two different materials, a p-type and an n-type material, for efficient charge separation, C<sub>60</sub> fullerene derivatives, which are generally used as the n-type material, have weak optical absorption in the visible and near infrared (NIR) region because of their high symmetry. To compensate for this optical absorption problem with C<sub>60</sub> derivatives, C<sub>70</sub> and its derivatives, which exhibit stronger optical absorption owing to their lower symmetry [12], have been frequently used as the n-type material.[13-15] However, C<sub>70</sub> and its derivatives are more expensive than C<sub>60</sub> and its

derivatives, which are already costly enough, because pristine C<sub>70</sub> is only obtained as a by-product of C<sub>60</sub> production. Using C<sub>70</sub> and its derivatives, instead of C<sub>60</sub>, to pursue higher PCE would, therefore, not be commercially viable. Another way to improve absorption efficiencies of the n-type layer in the visible-to-NIR region is, therefore, required. From the viewpoint of efficient charge separation and collection, fullerene derivatives are indispensable for forming the p/n heterojunction, so, it might seem that there is no practical solution to the problem described.

However, we have recently demonstrated the use of two p-type layers with complementary optical absorption properties.[16] Interlayer excitation transfer (ET) between the two layers leads to a relay of excitonic energies to the p/n junction, resulting in the sensitization of the organic PV. If the same system could be adopted for n-type materials, it would successfully allow the indispensable fullerene-based n-type layer system to be given higher optical densities. Thus, costly fullerene-based materials would not be required to achieve higher optical absorptions. In addition, it would probably be possible to reduce the amount of C<sub>60</sub> used because the thin C<sub>60</sub> layer in the n-type material is only used for charge separation. Therefore, it is necessary to explore the possibility of creating a light-harvesting n-type material incorporating fullerene-based organic PV cells to compensate for the fullerenes' weak optical absorption.

Here, we demonstrate that N,N'-diphenylperylene tetracarboxylic diimide (PTCDI-Ph, see Fig. 1a) can work as an n-type sensitizing layer for the indispensable C<sub>60</sub> n-type layer when the PTCDI-Ph layer is placed between the C<sub>60</sub> layer and the metal anode, which requires a thin bathocuproine (BCP) buffer layer, as shown in Fig. 1b.

## 2. Experimental

Figure 1b shows a schematic of the device structure used in the study, and Fig. 1a shows the chemical structures of the materials used. In this study we employed a (thiophene/phenylene) co-oligomer,  $\alpha,\omega$ -bisbiphenyl-*ter*-thiophene (BP3T), as the p-type material instead of more commonly used materials such as copper phthalocyanine (CuPc). This is because we aimed to determine exactly how the PTCDI-Ph layer works in organic photovoltaic devices. PTCDI-Ph (Dainichiseika Color & Chemicals), BP3T (Sumitomo Seika Industries), C<sub>60</sub> (Frontier Carbon), and BCP (TCI) were purified using temperature-gradient train sublimation with an Ar gas flow before use. We prepared the devices by depositing several materials sequentially onto commercially available indium–tin–oxide (ITO) coated glass substrates, which had a sheet resistance of 15 Ω/square. The substrates were first washed with aqueous detergent, pure water, and 2-propanol with ultrasonification and then treated with O<sub>2</sub> plasma at 50 W for 5 min. We prepared a poly(3,4-ethylenedioxythiophene) poly(styrenesulfonate) (PEDOT:PSS) layer on the substrates by spin-coating with a commercially available formula (Clevios P AI 4083, H.C. Starck), before depositing several organic layers by thermal evaporation under vacuum (<2.0 × 10<sup>-4</sup> Pa) at the rate of 0.5 Å/s. Finally, the aluminum electrode was prepared on top of the organic layer stack by thermal evaporation in a vacuum, at the rate of 10 Å/s. Active areas of the cells were approximately 6 mm<sup>2</sup>. We transferred the devices produced into a highly inert glove box (O<sub>2</sub> concentration 5 ppm, dew point <-50 °C) with no exposure to ambient conditions, and then mounted them in a small chamber, which had a quartz window, in the glove box. A source meter (Keithley, 2410) was used to measure the current density versus voltage (*J*–*V*) curves with 100 mW/cm<sup>2</sup> air mass 1.5 global (AM1.5G) artificial

solar light irradiation from a Newport Oriel solar simulator (Model 91160) with an AM1.5G filter (Newport Oriel, 81088) and a light intensity stabilizer (Newport Oriel, Model 68945). The irradiation power density was measured with a pyroelectric optical power meter (Ophir, P3). We recorded the incident photon–electron conversion efficiency (IPCE) spectra of the devices with a source meter (Keithley 2400) under monochromatic light irradiation from a light source (Bunko Keiki SM-25A). The intensity of the monochromatic light was measured for each wavelength with a calibrated silicon photodiode (Hamamatsu Photonics S1337-1010BQ). Absorption spectra of the thin-film samples were recorded with a Shimadzu spectrophotometer (UV-9150). Sample films were deposited by thermal evaporation on quartz substrates. The PTCDI-Ph highest occupied molecular orbital (HOMO) energy was determined with a photoelectron emission yield spectrometer (Riken Keiki AC-3). The optical band gap was equal to the spectral onset of an absorption spectrum. The onset was determined from the cross point between the tangent line at the lower-wavelength-side inflection point of the first absorption peak and the baseline (see Fig. 2). The lowest unoccupied molecular orbital (LUMO) energy was then estimated to be the difference between the HOMO energy and the optical bandgap.

### 3. Results and Discussion

Figure 3 shows  $J$ – $V$  curves of the cells with different thicknesses of the PTCDI-Ph layer—0 to 40 nm. At first, we found that a BP3T and C<sub>60</sub> heterojunction worked well because the  $J$ – $V$  curve of the non-PTCDI-Ph cell had a good shape. The shortcut current density ( $J_{SC}$ ) of 1.9 mA/cm<sup>2</sup> for the non-PTCDI-Ph cell was relatively small. This is because BP3T has strong optical absorption only in the blue to ultraviolet

light regions, as shown in Fig. 2. However, the fill factor (FF), 0.64, for the cell was relatively large, and this is consistent with the good hole transporting properties of BP3T.[17] The open circuit voltage ( $V_{OC}$ ), 0.51 V, was higher than that of conventional CuPc/C<sub>60</sub> PV cells (*ca.* 0.48 V) [16] because the BP3T HOMO level, -5.28 eV, is smaller than that of CuPc (-5.10 eV), as shown in Fig. 1c. Such  $V_{OC}$  tendencies are frequently seen in organic PV.[18]

When we introduced the PTCDI-Ph layer between the C<sub>60</sub> and BCP layers, the  $J-V$  curves were dramatically altered depending on the thickness of the PTCDI-Ph layer, as is clearly shown in Fig. 3. The most important point is that the  $J_{SC}$  increased to 3.4 mA/cm<sup>2</sup> when the thickness was 30 nm. We immediately realized from this that electrons can move in the PTCDI-Ph layer. This makes sense from the standpoint of the n-type organic transistor behavior of PTCDI-Ph [19] and other PTCDI derivatives.[20-24] However,  $J_{SC}$  was lower for the 40-nm thick layer than for the 30-nm thick layer. Note that the non-BP3T cell exhibited much worse performance than the others with the PTCDI-Ph layers, which indicates that the BP3T/C<sub>60</sub> junction mainly causes charge separation in the cells comprising BP3T, C<sub>60</sub>, and PTCDI-Ph.

Figure 4 shows the IPCE spectra of the cells with different PTCDI-Ph thicknesses. The IPCE spectrum for the non-PTCDI-Ph cell seems to be based on the optical absorption of the C<sub>60</sub> layer because of the similarities between the spectrum and the C<sub>60</sub> absorption coefficient spectrum shown in Fig. 2, which is consistent with the thickness of the BP3T layer (10 nm). The optical absorption of the BP3T layer contributes to the absorption below about 400 nm.

Figure 4 also clearly shows that the IPCE values at higher wavelengths than 400 nm increased with thickness of the PTCDI-Ph layer. For example, the IPCE at 500

nm increased as the PTCDI-Ph layer increased up to 30 nm thick. However, the IPCE at 500 nm decreased for the 40 nm thick layer, and the IPCE at wavelengths below 400 nm were small, especially for layers more than 30 nm thick. As shown in Fig. 2, PTCDI-Ph gives strong optical absorption around 400–600 nm, with peaks at 568, 538, and 458 nm, and a shoulder at 485 nm. Looking at the IPCE spectra for the 30 nm and 40 nm thick PTCDI-Ph cells shown in Fig. 4, it appears that a small but clear shoulder appeared around 550 nm. It is clear, therefore, that the optical absorption of PTCDI-Ph in the thick (30 and 40 nm) PTCDI-Ph cells contributed to their photon–electron conversions. In the cell design, the PTCDI-Ph layer has no direct contact with the BP3T layer, which is the p-type layer, and the 40-nm thick C<sub>60</sub> layer ensures lack of direct contact. As we have already reported, for organic PV cells with several combinations of different p-type materials, [16] ET occurs from the PTCDI-Ph to the C<sub>60</sub> layer, and charge separation finally occurs at the BP3T/C<sub>60</sub> interface. The PTCDI-Ph bandgap is larger than that of C<sub>60</sub>, as shown in Fig. 1c. A larger PTCDI-Ph bandgap would drive the ET. This finding indicates that our organic PV sensitizing concept, based on interlayer ET, can work even with combinations of n-type materials.

When the thickness of the PTCDI-Ph layer was 10 and 20 nm, sensitization from PTCDI-Ph, which appeared as the shoulder around 550 nm was not observed. However, IPCE sensitizations were observed and the improvements in  $J_{SC}$  also occurred. We think that the thin PTCDI-Ph layers work as an optical buffer layer. That is, the insertion of the PTCDI-Ph layer made the C<sub>60</sub> layer farther from the Al anode, and, in other words, the C<sub>60</sub> layer became closer to the first antinode of the standing waves formed from the incident light and reflected light from the anode. As a result, the optical absorption of the C<sub>60</sub> layer and the IPCE were enhanced. Examining the IPCE spectrum

for the thick PTCDI-Ph layers (for example, 40 nm) in Fig. 4 closely, another small but clear shoulder can be seen around 625 nm, and this shoulder could also be observed in all of the IPCE spectra. The C<sub>60</sub> absorption spectrum contains a similar shoulder at the same wavelength. PTCDI-Ph has no optical absorption in this wavelength region, so an optical buffer effect was even more marked, even though the C<sub>60</sub> optical absorption in this region is very weak. In addition, decreases in the IPCE below 400 nm result from the same buffer effect because of the dependence of the antinode position on the light wavelength. Transfer matrix analyses [25, 26] of light standing waves in the cells in the Supplementary Information support this discussion (Fig. S1) as well as the lack of a shoulder in IPCE due to PTCDI-Ph in thinner PTCDI-Ph cells (Fig. S2).

The extracted parameters from the  $J$ - $V$  curves,  $J_{SC}$ ,  $V_{OC}$ , and FF, are summarized in Figure 5. The  $J_{SC}$  calculated from the IPCE spectra and the ideal AM1.5G solar spectrum (100 mW/cm<sup>2</sup>) are also shown in the figure. Although the exact  $J_{SC}$  values at each thickness are systematically different, probably because of differences between the artificial solar simulator spectrum and the ideal spectrum, the thickness dependence tendencies are the same. This means that the changes in  $J_{SC}$  in Fig. 3 are consistent with those in the IPCE spectra. The FFs were almost the same using PTCDI-Ph layer thicknesses between 0 and 20 nm, which means PTCDI-Ph has no influential electron barrier at either the C<sub>60</sub>/PTCDI-Ph interface or the PTCDI-Ph/BCP interface. The PTCDI-Ph LUMO level is -4.55 eV, which is very close to the C<sub>60</sub> LUMO (-4.5 eV), so no influential barrier appeared. However, the thicker PTCDI-Ph layer led to a slight decrease in FF, and we suppose that it was influenced by the PTCDI-Ph electron transporting properties.[19] The  $V_{OC}$  values also depended on the PTCDI-Ph layer thickness. One of the possible reasons must be the  $J_{SC}$  dependence on

$V_{OC}$ ; however,  $V_{OC}$  was almost saturated at the PTCDI-Ph thickness of 40 nm, where  $J_{SC}$  decreased. Therefore, another reason has to exist and further studies are required.

Figure 6 shows the  $J$ - $V$  curves of the cells with a  $C_{60}$  layer of a reduced thickness (10 nm) and no  $C_{60}$  layer. The cells have a 30-nm-thick PTCDI-Ph layer, optimized in the former section, and the cell structures are presented in the figure inset. What we first deduce from this figure is that the  $C_{60}$  layer is indispensable for efficient current generation even if its thickness is low. That is, the 10-nm-thick  $C_{60}$  layer cell exhibited a  $J_{SC}$  of  $2.4 \text{ mA/cm}^2$ , although the non- $C_{60}$  cell showed a  $J_{SC}$  of only  $0.33 \text{ mA/cm}^2$ . Furthermore, a comparison of the  $J_{SC}$  of the 10-nm-thick  $C_{60}$  layer cell with that of the 40-nm-thick  $C_{60}$  layer cells (Fig. 3) shows that the  $J_{SC}$  of  $2.4 \text{ mA/cm}^2$  is larger than that of the cells with 0- and 10-nm-thick PTCDI-Ph layers. The total thickness (40 nm) of the  $C_{60}$  (10 nm) and PTCDI-Ph (30 nm) layers in the cell (Fig. 6) is the same as the thickness of the  $C_{60}$  layer of the 0-nm-thick PTCDI-Ph cell (Fig. 3). An approximately 30% increase in  $J_{SC}$  from  $1.9 \text{ mA/cm}^2$  (BP3T/40-nm- $C_{60}$ ) to  $2.4 \text{ mA/cm}^2$  (BP3T/10-nm- $C_{60}$ /30-nm-PTCDI-Ph) indicated that this n-type material combination of  $C_{60}$  and PTCDI-Ph could successfully reduce the amount of the expensive  $C_{60}$  used, and a thin  $C_{60}$  layer was indispensable for efficient charge separation. In summary, PTCDI-Ph could work as a light-harvesting n-type material incorporating  $C_{60}$ -based cells to compensate for  $C_{60}$ 's weak optical absorption. We demonstrated that this concept worked well in stacked-layer organic PV cells, but this might also work in bulk heterojunction (BHJ)-architecture-based organic PV cells [7], where the active layer is a mixture of a p-type material and a fullerene derivative. This is because the additional n-type material layer, which is placed between the BHJ layer and the metal anode, could work as a sensitizing buffer layer.

## 4. Conclusion

We have demonstrated that PTCDI-Ph could work as an n-type sensitizing layer for the C<sub>60</sub> n-type layer when the PTCDI-Ph layer is placed between the C<sub>60</sub> layer and the aluminum anode. This indicated that interlayer ETs, for relaying excitonic energies to the p/n junction, worked well in n-type layer systems. It was also demonstrated that the amount of C<sub>60</sub> used in these layers could be reduced while maintaining a higher  $J_{SC}$ , and only a thin C<sub>60</sub> layer was required for effective charge separation.

**Acknowledgements:** This work was supported by the JST PRESTO program (Photoenergy Conversion Systems and Materials for the Next Generation Solar Cells).

## References

- [1] S. R. Forrest, *Nature* **428** (2004) 911.
- [2] F. C. Krebs, T. Tromholt, M. Jorgensen, *Nanoscale* **2** (2010) 873.
- [3] R. Fitzner, E. Reinold, A. Mishra, E. Mena-Osteritz, H. Ziehlke, C. Körner, K. Leo, M. Riede, M. Weil, O. Tsaryova, A. Weiß, C. Uhrich, M. Pfeiffer, P. Bäuerle, *Adv. Funct. Mater.* **21** (2011) 897.
- [4] T. Kaji, M. Zhang, S. Nakao, K. Iketaki, K. Yokoyama, C. W. Tang, M. Hiramoto, *Adv. Mater.* **23** (2011) 3320.
- [5] X. Xiao, G. Wei, S. Wang, J. D. Zimmerman, C. K. Renshaw, M. E. Thompson, S. R. Forrest, *Adv. Mater.* **24** (2012) 1956.

- [6] M. A. Green, K. Emery, Y. Hishikawa, W. Warta, E. D. Dunlop, Progress in Photovoltaics: Research and Applications **20** (2012) 12.
- [7] C. J. Brabec, S. Gowrisanker, J. J. M. Halls, D. Laird, S. Jia, S. P. Williams, Adv. Mater. **22** (2010) 3839.
- [8] Y. Liang, Z. Xu, J. Xia, S.-T. Tsai, Y. Wu, G. Li, C. Ray, L. Yu, Adv. Mater. **22** (2010) E135.
- [9] H. Zhou, L. Yang, A. C. Stuart, S. C. Price, S. Liu, W. You, Angewandte Chemie **123** (2011) 3051.
- [10] L. Dou, J. You, J. Yang, C.-C. Chen, Y. He, S. Murase, T. Moriarty, K. Emery, G. Li, Y. Yang, Nat Photon **6** (2012) 180.
- [11] C. W. Tang, Appl. Phys. Lett. **48** (1986) 183.
- [12] J. W. Arbogast, C. S. Foote, J Am Chem Soc **113** (1991) 8886.
- [13] M. M. Wienk, J. M. Kroon, W. J. H. Verhees, J. Knol, J. C. Hummelen, P. A. van Hal, R. A. J. Janssen, Angew. Chem. Int. Ed. **42** (2003) 3371.
- [14] P. Vemulamada, G. Hao, T. Kietzke, A. Sellinger, Org. Electron. **9** (2008) 661.
- [15] S. Pfuetzner, J. Meiss, A. Petrich, M. Riede, K. Leo, Appl. Phys. Lett. **94** (2009) 223307.
- [16] M. Ichikawa, E. Suto, H.-G. Jeon, Y. Taniguchi, Org. Electron. **11** (2010) 700.
- [17] K. Nakamura, M. Ichikawa, R. Fushiki, T. Kamikawa, M. Inoue, T. Koyama, Y. Taniguchi, Jpn J. Appl. Phys. **43** (2004) L100.
- [18] M. C. Scharber, D. Mühlbacher, M. Koppe, P. Denk, C. Waldauf, A. J. Heeger, C. J. Brabec, Adv. Mater. **18** (2006) 789.
- [19] G. Horowitz, F. Kouki, P. Spearman, D. Fichou, C. Nogues, X. Pan, F. Garnier, Adv. Mater. **8** (1996) 242.

- [20] S. Tatemichi, M. Ichikawa, T. Koyama, Y. Taniguchi, *Appl. Phys. Lett.* **89** (2006) 112108.
- [21] H.-G. Jeon, J. Hattori, S. Kato, N. Oguma, N. Hirata, Y. Taniguchi, M. Ichikawa, J. *Appl. Phys.* **108** (2010) 124512.
- [22] H.-G. Jeon, Y. Yokota, J. Hattori, N. Oguma, N. Hirata, T. Suzuki, M. Ichikawa, *Appl. Phys. Express* **5** (2012) 041602.
- [23] Y. Wen, Y. Liu, C.-a. Di, Y. Wang, X. Sun, Y. Guo, J. Zheng, W. Wu, S. Ye, G. Yu, *Adv. Mater.* **21** (2009) 1631.
- [24] C. Huang, S. Barlow, S. R. Marder, *J. Org. Chem.* **76** (2011) 2386.
- [25] W. N. Hansen, *J. Opt. Soc. Am.* **58** (1968) 380.
- [26] P. Peumans, A. Yakimov, S. R. Forrest, *J. Appl. Phys.* **93** (2003) 3693.

### **Figure Captions**

Figure 1. (a) The structures of the chemicals used and their abbreviations, (b) the sectional cell structure, and (c) energy diagram of the PV cell proposed in this study.

Figure 2. Absorption coefficient (ratio of absorbance and film thickness) spectra of each thin film.

Figure 3. Current density *versus* voltage characteristics of cells with different PTCDI-Ph thicknesses. The current density-voltage curve of a cell with ITO/PEDOT:PSS/C<sub>60</sub>(40 nm)/PTCDI-Ph(30 nm)/BCP/Al structure is also shown by the dashed line.

Figure 4. IPCE spectra of cells with different PTCDI-Ph thicknesses.

Figure 5. PTCDI-Ph thickness dependences of  $J_{SC}$ ,  $V_{OC}$ , and FF. Two  $J_{SCS}$ , (■) measured and (□) calculated (see text), are displayed.

Figure 6. Current density *versus* voltage characteristics of cells with different C<sub>60</sub> thicknesses (inset: structure of cells).

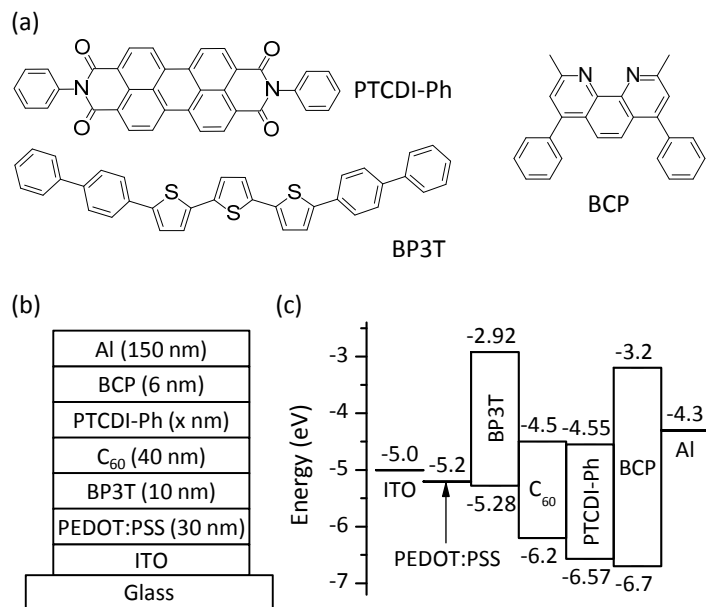


Figure 1. (a) The structures of the chemicals used and their abbreviations, (b) the sectional cell structure, and (c) energy diagram of the PV cell proposed in this study.

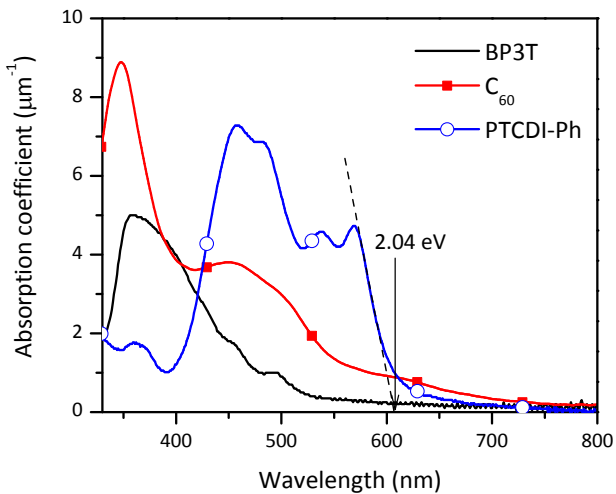


Figure 2. Absorption coefficient (ratio of absorbance and film thickness) spectra of each thin film.

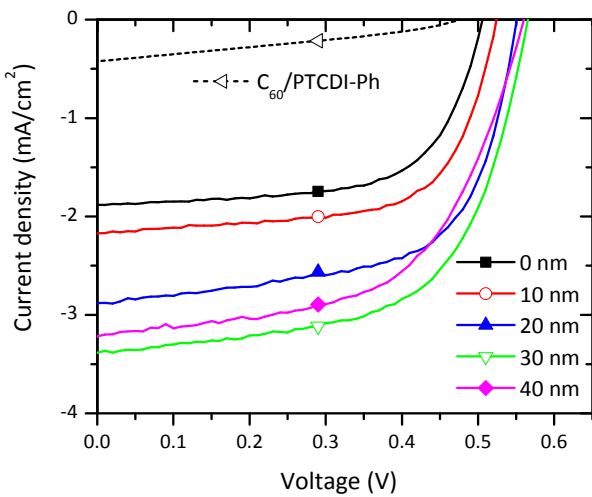


Figure 3. Current density *versus* voltage characteristics of cells with different PTCDI-Ph thicknesses. The current density-voltage curve of a cell with ITO/PEDOT:PSS/C<sub>60</sub>(40 nm)/PTCDI-Ph(30 nm)/BCP/Al structure is also shown by the dashed line.

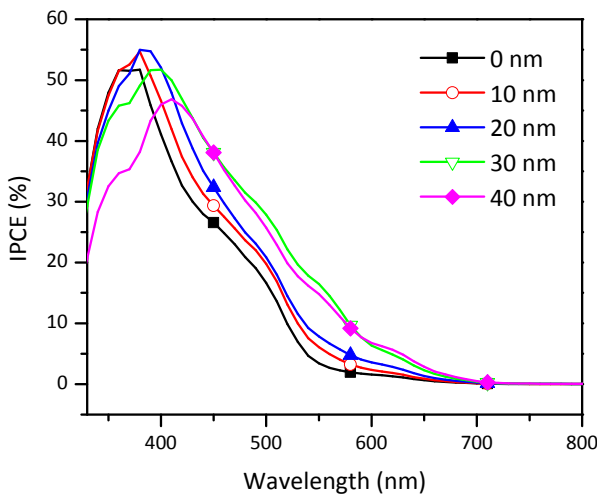


Figure 4. IPCE spectra of cells with different PTCDI-Ph thicknesses.

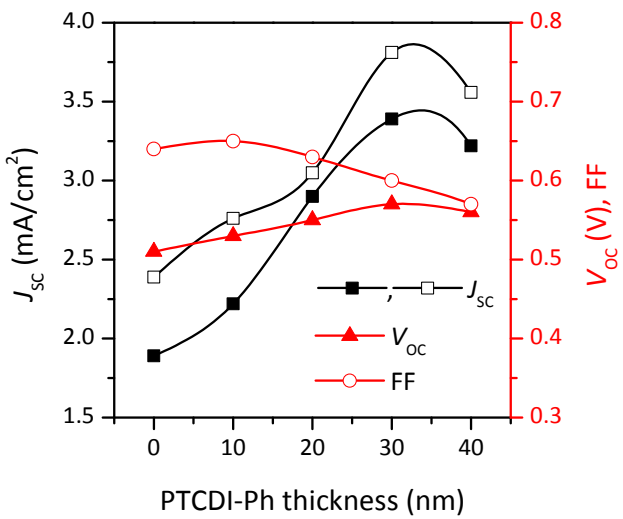


Figure 5. PTCDI-Ph thickness dependences of  $J_{SC}$ ,  $V_{oc}$ , and FF. Two  $J_{SC}$ s, ( $\blacksquare$ ) measured and ( $\square$ ) calculated (see text), are displayed.

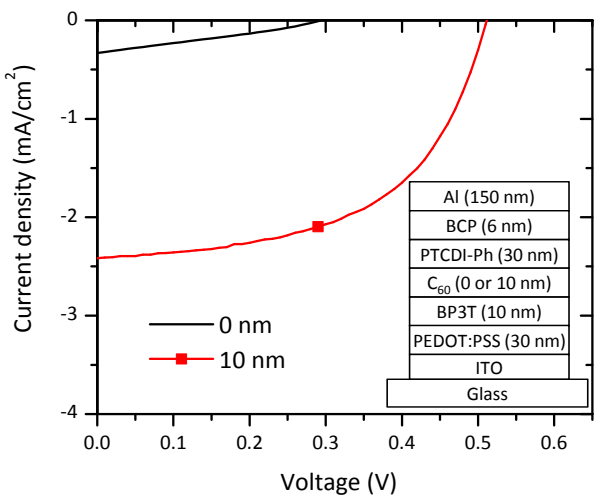


Figure 6. Current density *versus* voltage characteristics of cells with different  $C_{60}$  thicknesses (inset: structure of cells).

## Supplementary Information

### **N,N'-Diphenylperylene Diimide Functioning as a Buffer Material for a Metal Anode and a Sensitizing Light Absorber for Organic Thin-Film Solar Cells**

Musubu Ichikawa, Shinya Deguchi, Takashi Onoguchi, Hyeon-Gu Jeon, Gilles D. R. Banoukepa

#### *Transfer Matrix Analysis of Light Standing Wave in Cells*

The transfer matrix method is widely used for analyzing light standing waves because of optical interference in organic thin-film solar cells. This method requires the optical constant (complex refractive index) of the materials at each wavelength. However, there are no data regarding the optical constant, in particular, the refractive index of BP3T and PTCDI-Ph. Therefore, in the following analysis, we assumed their refractive indexes to be 2, although their extinction coefficients were estimated from the absorption spectra of their thin films. The analysis results are somewhat erroneous; however, they are qualitatively correct because an assumed refractive index of 1.8 gave almost the same results. Table S1 summarizes all the optical parameters used.

The standing wave fields in the cells at wavelengths of 380 and 630 nm are shown in Fig. S1. The 40-nm-thick PTCDI-Ph layer forced the placement of the C<sub>60</sub> layer at the first *antinode* of the 630 nm wavelength light and the first *node* of the 380 nm wavelength light. On the other hand, the 10-nm-thick PTCDI-Ph layer led the C<sub>60</sub> layer to shift toward the first antinode of the 380 nm wavelength light. Furthermore, no clear shoulder in the IPCE spectra due to PTCDI-Ph was observed in the cells with the thinner (10 nm and 20 nm) PTCDI-Ph layers. The transfer matrix analysis also depicted light standing wave fields at a wavelength of 550 nm, as shown in Fig. S2. The first

antinode of the standing wave at 550 nm is located nearly at the interface of BP3T and C<sub>60</sub> and far from the 10-nm-thick PTCDI-Ph layer in the cell. This small overlap between the layer and the field caused no apparent sensitization in IPCE because of PTCDI-Ph. A thicker PTCDI-Ph could shift the antinode toward the PTCDI-Ph layer and the sensitization to become apparent.

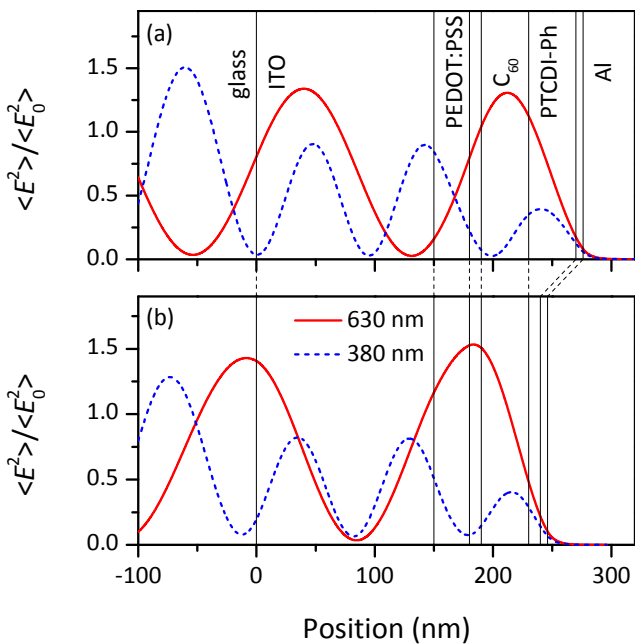


Fig. S1. Normalized time-averaged squared electric field standing waves of light at 380 and 630 nm in the cells comprising a PTCDI-Ph layer: (a) 40 nm and (b) 10 nm thick.

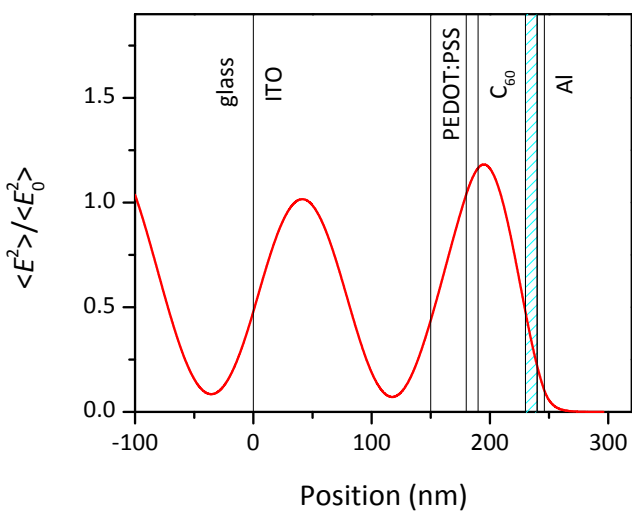


Fig. S2. Normalized time-averaged squared electric field standing waves of light at 550 nm in the cell with a 10-nm-thick PTCDI-Ph layer. The position of the PTCDI-Ph layer is depicted with the cyan hatched area.

Table S1. Complex refractive indexes ( $n + ik$ ) of the materials at three wavelengths.

Material	Refractive indexe					
	380 nm		550 nm		630 nm	
	<i>n</i>	<i>k</i>	<i>n</i>	<i>k</i>	<i>n</i>	<i>k</i>
Glass <sup>a</sup>	1.56	0	1.52	0	1.51	0
ITO <sup>a</sup>	2.01	0.012	1.81	0.003	1.73	0.005
PEDOT:PSS <sup>a</sup>	1.54	0.018	1.48	0.04	1.43	0.062
BP3T <sup>b</sup>	2	0.323	2	0.035	2	0
C <sub>60</sub> <sup>c</sup>	2.41	0.353	2.22	0.14	2.14	0.091
PTCDI-Ph <sup>b</sup>	2	0.089	2	0.426	2	0
BCP <sup>d</sup>	1.85	0.01	1.72	0	1.7	0
Al <sup>e</sup>	0.435	4.61	0.98	6.68	1.34	7.58

<sup>a</sup>H. Hoppe, N. S. Sariciftci, D. Meissner, Mol. Cryst. Liq. Cryst. **385** (2002) 113.

<sup>b</sup>The real parts of the refractive indexes of the materials were assumed to be 2, and the imaginary parts were calculated from the absorption coefficients ( $\alpha$ ) at each wavelength ( $\lambda$ ) (Fig. 2) on the basis of equation  $k = \alpha\lambda \ln 10/(4\pi)$ .

<sup>c</sup>L. A. A. Pettersson, L. S. Roman, O. Inganäs, J. Appl. Phys. **86** (1999) 487.

<sup>d</sup>Z. T. Liu, C. Y. Kwong, C. H. Cheung, A. B. Djurišić, Y. Chan, P. C. Chui, Synth. Met. **150** (2005) 159.

<sup>e</sup>D. R. Lide, Handbook of Chemistry and Physics. 83rd ed.; CRC Press: 2002.